



City Research Online

City, University of London Institutional Repository

Citation: Marichal, N., Tomas-Rodriguez, M., Hernandez, A., Castillo, S. & Campoy, P. (2013). Vibration reduction for vision systems on board UAV using a neuro-fuzzy controller. *Journal of Vibration and Control*, 20(15), pp. 1-12. doi: 10.1177/1077546313479632

This is the accepted version of the paper.

This version of the publication may differ from the final published version.

Permanent repository link: <https://openaccess.city.ac.uk/id/eprint/12547/>

Link to published version: <https://doi.org/10.1177/1077546313479632>

Copyright: City Research Online aims to make research outputs of City, University of London available to a wider audience. Copyright and Moral Rights remain with the author(s) and/or copyright holders. URLs from City Research Online may be freely distributed and linked to.

Reuse: Copies of full items can be used for personal research or study, educational, or not-for-profit purposes without prior permission or charge. Provided that the authors, title and full bibliographic details are credited, a hyperlink and/or URL is given for the original metadata page and the content is not changed in any way.

City Research Online:

<http://openaccess.city.ac.uk/>

publications@city.ac.uk

Vibration reduction for vision systems on board UAV using a neuro-fuzzy controller

G. Nicolás Marichal ¹, María Tomás-Rodríguez ², Ángela Hernández ¹, Salvador Castillo-Rivera ², P. Campoy ³

¹ Departamento de Ingeniería de Sistemas y Automática,
Arquitectura y Tecnología de Computadoras, Universidad
de La Laguna, Spain

² The Engineering and Mathematics Department. City
University, United Kingdom

³ Grupo de Visión por Computadoras. Universidad
Politécnica de Madrid, Spain

Corresponding autor:

Ángela Hernández López, Facultad de Física,
C/Astrofísico Francisco Sánchez s/n 38200, La Laguna,
España

EMail: angela@isaatc.ull.es;

Abstract:

In this paper, an intelligent control approach based on Neuro-Fuzzy systems performance is presented with the objective of counteracting the vibrations that affect the low-cost vision platform onboard an unmanned aerial system of rotating nature.

A scaled dynamical model of a helicopter is used to simulate vibrations on its fuselage. The impact of these vibrations on the low-cost vision system will be assessed and an intelligent control approach will be derived in order to reduce its detrimental influence.

Different trials that consider a Neuro-Fuzzy approach as a fundamental part of an intelligent semi-active control strategy have been carried out. Satisfactory results have been achieved compared to those obtained by means of vibration reduction passive techniques.

Keywords

Vibration, control, neuro-fuzzy, model, intelligent.

Introduction

Rotary-wing unmanned aerial vehicle (UAV) systems are greatly affected by vibrations frequently originated on its rotors. The characteristics (frequency and amplitude) of these vibrations often lead towards detrimental performance of the vehicle's on-board systems. Vision systems onboard UAVs are subject to high dynamic vibrations from several sources, such as the engine or the rotor blades. These multi-modal spectrum vibrations cause a significant degradation in the quality of the captured images, especially in small size aircrafts. In these cases, there is a need for reducing the vibration influence over the captured images by designing and implementing an isolation system. The problem of vibration isolation can be tackled in various ways.

Several studies have been developed in order to compare different techniques (Jansen et al. 1999), (Miller et al. 1988). Passive vibration reduction devices are the most classical methods, consisting of springs that support the load, and dampers that dissipate energy. These systems require no external power or computer processes for operation. Once the isolation mechanism is installed, its properties cannot be modified; therefore **the major disadvantage of passive vibration reduction systems** is the lack of adaptability to changes during flight operations. On the other hand, active control techniques have the capability to adapt whilst changing flight conditions, overcoming in this way one of the passive methods major drawbacks. Nevertheless, active control presents an important limitation as it requires an external power source. Since the 70's, the advantages of using semi-active devices have been addressed in several studies (Karnopp et al. 1974), (Rakheja et al. 1985, 1986). Years of studies have shown that these methods continue improving since they have set better techniques (Alanoly et al. 1987), (Wu et al. 1997). In fact, they do have low energy requirement which is a desirable characteristic in the UAVs systems environment. **Mainly, semi-active isolation systems consist of** a variable damping device such that the damping properties can be modified in real time **in order to provide significant vibration reduction** in onboard vision systems. Therefore, this adaptive damping methodology is especially useful for the cases where spectrum is of the multi-modal nature.

In this article, an intelligence control strategy based on a semi-active approach is presented in order to improve the performance of a low-cost vision system onboard a UAV. In the following section, a description of the simulation model of the helicopter prototype used for vibration generation is given. The next one explains the simulation environment where the semi-active control strategy is applied on the vision system. Next, it is focused on the description and application of an Adaptive Neuro-Fuzzy Inference System as control approach. Finally, the results obtained are shown. Furthermore conclusions and suggestions of further work are presented in the last section.

Helicopter simulation model

Rotorcrafts are mechanically complex, with many bodies, several degrees of freedom and general motions in three dimensions possible. Since the 60's, the modeling of helicopter dynamics has been technically challenging. In the late 80's, improving understanding and advances in computation allowed progress to accelerate. Nowadays, studies in this area are extremely wide, as they entail amongst others, advanced methods in computational fluid dynamics (CFD) and flexible multibody dynamics (Naramore, 1995). The majority of existing models in the literature tend to be relaxed in reflecting the full set of dynamics involved in helicopter behavior. Several of the existing results to date have been based on linearised models (Garrad et al. 1990), (Kienitz et al. 1990). Most of them consider linear time-invariant models only in the case of a hovering rotor,

whilst in forward flight such dynamics turn out to be time-periodic (Bittanti et al. 1996), (Johnson, 1980) with period equal to the rotor revolution period. On the other hand, there exist some nonlinear descriptions of helicopter dynamics but only for reduced order models (Kaloust, 1997) or without taking into consideration the interaction of the main rotor with the fuselage (Verdult et al. 2004). The model here presented is a realistic nonlinear model of the fundamental dynamics of an articulated rigid-bladed rotorcraft. One of the advantages of this model is that it gives an accurate representation of the complex system's dynamics.

It consists of a 6 DOF (Degrees of freedom) fuselage plus an articulated main rotor consisting of a set of four blades and a tail rotor with two blades. This model does take into account highly coupled nonlinear dynamic terms and no approximations are taken, in the same line as the analytical results published in (Decker et al. 1982), (Heffley et al. 1988), (Padfield, 1996) which constituted the starting point for a significant number of helicopter flight simulations, in military and research fields.

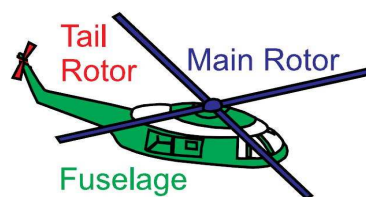


Figure1. Helicopter subsystems: Main Rotor, Fuselage and Tail Rotor.

A helicopter can be defined in a very general way as an aircraft that uses rotating wings to provide lift, propulsion and control.

The *fuselage* is the rotorcraft's main body section that holds crew and passengers or cargo. Its degrees of freedom are the lateral and longitudinal translation in the horizontal plane (X-Y axis), vertical translation (Z axis) and rotation about these same axes corresponding to yaw, feather and roll.

The *main rotor* generates the thrust that supports the weight and controls the aircraft. It transfers prevailing aerodynamic forces and moments from the rotating blades to the non-rotating frame (fuselage); a conventional rotor consists of two or more identical equally spaced blades attached to a central hub. The blades are kept in uniform rotational motion (rotational speed Ω) by a shaft torque from the engine. A common design solution adopted in the development of the helicopter is to use hinges at the blades roots that allow free motion of the blade normal to and in the plane of the disk. The rotor considered in this article is an articulated rotor; the blades are attached to the hub by flap β , lag ζ and, feather θ hinges, (see figure 2).

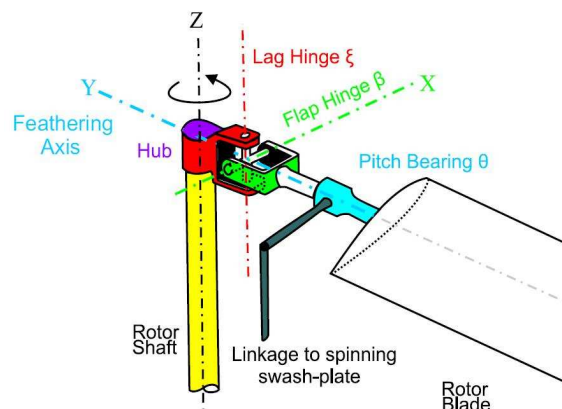


Figure 2. Sequence of hinges in an articulated rotor with corresponding degrees of freedom.

The most common of these hinges is the flapping hinge which allows the blade to flap, this is, to rise and fall in similar manner to the beating of a bird's wing. In some cases, the flap hinge is substituted by a region of structural flexibility at the root of the blade. The flapping hinge is usually at a short distance from the rotor center-line, termed "offset flapping hinge". Centrifugal stiffening due to rotor spin is vital to a blade's integrity in helicopter flight (<http://avia.russian.ee>). A spinning blade which also flaps, experiences large Coriolis moments about the vertical, lag-hinge axes. The lag hinge provides stress-relief at the blade root. This degree of freedom produces blade motion in the disk plane. The lagging angle is considered to be positive when opposite the direction of rotation of the rotor, as produced by the blade drag forces.

Blade feathering motions, θ (also known as angle of attack) need to be controlled to regulate the aerodynamic lift developed and, in forward motion to allow the advancing blade to have a lower angle of incidence than the retreating blade and to thereby balance the lift across the craft's rotor plane. Feathering the blades simultaneously is referred to as *collective* feather control, whilst feathering them differentially is called *cyclic* feather control. Blade feathering control is achieved through linkage of the blade to a swash-plate, (see figure 2), the pilot having control of the height (collective) and angle (cyclic) of the plate through a joy-stick.

The helicopter fuselage tends to rotate in the direction opposite to the rotor blades. This torque effect on the fuselage is a direct result of the work/resistance of the main

rotor. The *tail rotor* of the helicopter is mounted on the tail of a single-rotor helicopter, perpendicular to the main rotor. It is used in order to counteract the torque and the yaw motion that the main rotor disk naturally produces. Two anti-torque pedals allow the pilot to compensate for torque variance by providing a means of changing pitch (angle of attack) of the tail rotor blades. This provides heading and directional control in hover and at low airspeeds.

In addition to counteracting torque, the tail rotor and its control linkage also allows control of the helicopter heading during flight. Application of more control than is necessary to counteract the torque will cause the nose of the helicopter to swing in the direction of pedal movement. To maintain a constant heading at a hover or during takeoff or approach, the pilot must use the antitorque pedals to apply just enough pitch on the tail rotor to neutralize torque and hold a slip if necessary. Heading control in forward trimmed flight is normally accomplished with cyclic control.

After introducing the main dynamical characteristics of a helicopter, the modeling aspects will be addressed in the following subsections.

Dynamical modelling tool: VehicleSim

VehicleSim (<http://www.carsim.com/>) is one of a number of multibody modeling systems currently in common use. The system has been used over a wide range of mechanical dynamic problems, mainly in connection with vehicle dynamics (Sharp et al. 2005, 2004), (Mousseau et al. 1992), (Sayers et al. 1999), (Tomás-Rodríguez et al.

2007) and it has provided the basis for the commercial simulation codes TruckSim, CarSim and BikeSim (<http://www.carsim.com/>). VehicleSim is a set of LISP macros (Steele et al. 1984), enabling the description of mechanical multibody systems, with possible addition of non-mechanical subsystems.

The output from VehicleSim takes one of several forms: (a) a Rich Text Format file containing the symbolic equations of motion of the system described; (b) a "C" language simulation program with appropriate data files containing parameter values and simulation run control parameters (or Simulink S-function); or (c) linear state-space equations in a Matlab "M-file" format that contains symbolic state-space A, B, C, D matrices for linear analysis. Once the model has been built, it becomes independent of VehicleSim and it can be executed at any time. VehicleSim commands are used to describe the components of the helicopter multibody system in a parent-child relationship according to their physical constraints and joints. The VehicleSim code is then used to generate a C simulation program, capable of computing general motions corresponding to specified initial conditions and external forcing inputs.

Simulations for vibrations generation

The complete dynamical helicopter model was implemented as described in section 2 (more details on modeling of this system can be found in (Tomás-Rodríguez et al. 2007) and (Tomás-Rodríguez et al. 2008)). The model parameters are as follows: the main rotor is composed of four blades each of mass $m_b=31.06$ Kg. The length of each main

rotor blade is $l_m = 4.91$ m and the rotational speed of the rotor is $\Omega_m = 44.4$ rad/s. The main rotor blades moments of inertia on the X and Z axis are $I_x = I_z = 62.4$ Kg·m² and the on the Y axis $I_y = 0.07488$ Kg·m², are the same for each blade. The fuselage mass is $m_f = 2200$ kg. The height of the rotor disk above the fuselage is $h = 1.48$ m. The tail rotor is composed of two blades each of mass $m_t = 6.212$ Kg. The length of each blade is $l_t = 0.982$ m and the rotational speed of the tail rotor is $\Omega_t = 222$ rad/s. The tail rotor blades moments of inertia on the X and Z axis are $I_x = I_z = 12.48$ Kg·m² and on the Y axis is $I_y = 0.015$ Kg·m², these are the same for each blade.

The fuselage is allowed 6 degrees of freedom, longitudinal, lateral and vertical along the axes X, Y, Z respectively and the corresponding rotations about these same axes. The acceleration of gravity is neglected for the purpose of these simulations as the object of study is the dynamic behavior of the various subsystems of the helicopter and the forces and accelerations that occur as a result of interactions and couplings between them.

In order to study the characteristics of the vibrations occurring in the fuselage due to the main rotor only, a simulation is carried out where the main rotor has an angular velocity of $\Omega_m = 44.4$ rad/s, and the tail rotor speed is fixed at $\Omega_t = 0$ rad/s. As the main objective at this stage is vibration generation, a mass imbalance is introduced artificially, this is, the mass of one of the main rotor blades is reduced to its half, this is,

$m_b=15.53$ kg, which will cause vibrations to appear and to be transmitted to the fuselage.

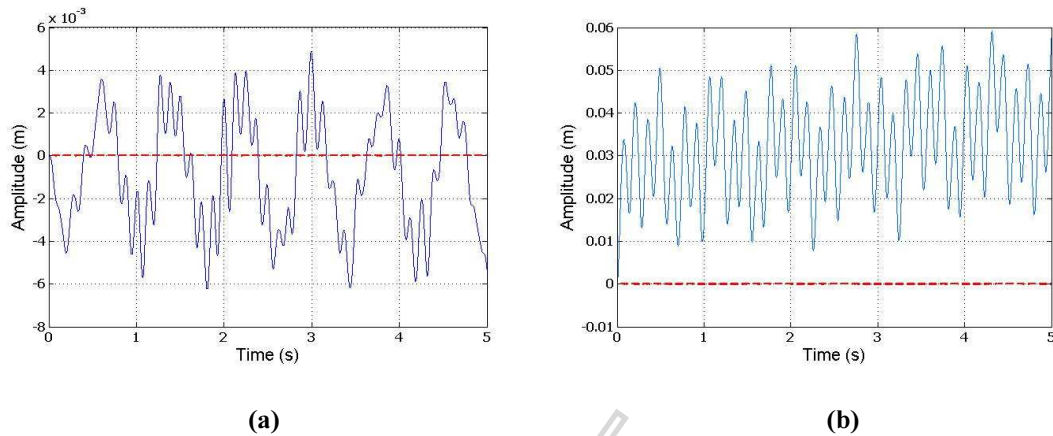


Figure 3: (a) Vibrations appearing in Z-axis (blue solid line) when main rotor blade mass imbalance is included in the simulation. (b) Vibrations appearing in Y-axis (blue solid line) when main rotor mass imbalance is included in the simulation. The red dotted line on both cases represents the fuselage steadiness when no mass imbalance is introduced.

In figure 3 the vibrations appearing on both Z and Y-axis are shown for a length of time of $T=5$ seconds. The simulations were run for a period of 50 seconds and the corresponding data were analyzed using a FFT (Fast Fourier Transform) algorithm. The main frequency component of the spectrum of vibrations appearing in the Z-axis was of $f=50.58$ rads/s, whilst the main frequency component of the vibrations appearing in the Y-axis had a frequency of $f=44.04$ rads/s. These range of frequencies agree with those predicted by the theory and will be used later on in this work in order to design the control algorithm that will isolate the vision system from these unwanted disturbances.

At this point, the knowledge on the expected frequencies allows us to narrow our attention to this particular range and to perform a more exhaustive analysis over the problematic frequencies.

Experimental set-up

The vision system is one of the most susceptible elements to suffer from detrimental effects of the vibrations produced by the helicopter. To study the magnitude of this effect, a dynamic platform SPT 200 SERVICITY has been modelled in Simulink/Simmechanics (<http://www.mathworks.com/products/simulink/>). This platform is designed to support a 0.9 kg camera and it has two servomotors incorporated which allow the change of the camera's yaw and pitch angles.

Figure 4 shows the dynamic platform mounted on the helicopter and Figure 5 shows a detail of the low-cost camera mounted on the platform.



Figure 4. Platform SPT 200 mounted on the helicopter



Figure 5. Detail of the vision mounted system on the platform

The platform consists of three parts: the base, an intermediate body, where the joint between both bodies allows displacement; and finally, a third body linked to the second one by a joint that allows pitch movements. Their Inertia matrices, centres of gravity and other geometry data have been calculated and included in the simulation.

Furthermore, a PID controller for each servomotor is also included, as well as the camera and a spring-mass system in order to account for the structural flexibility of the platform. Table 1 contains information relevant to the system's characteristics:

Mode	Natural Frequency (Hz)
1	6.7
2	5.7
3	4.5

Table 1: Undamped System's Characteristics

Since the purpose of this modelling is to test the behaviour of the camera under the vibration effect transmitted from the fuselage, an input block for these vibrations needs to be included. However, it should be noted that the methods used in this work are not limited to a particular dynamic platform, as it will be shown on the following section, the control algorithm is devised from a set of input vibration signals and output vibration signals.

Proposed control algorithm

The chosen method in order to decrease the vibration on the vision system is a semi-active approach technique; in particular, a spring-damper system is used where the damping coefficient value is a time-dependant, $C(t)$. This time dependency allows for an adaptive damping method as the transmitted vibrations to the platform change with time. This method requires an external agent that produces the change of the damping variable $C(t)$. An intelligent system that provides the adequate values for each situation has been designed for this purpose. For the control method design, we need to take into account that the performance of the semi-active device depends on the type of vibration to be damped, therefore it is reasonable to use the vibration frequencies appearing on the helicopter fuselage as inputs. In this paper, the frequency of vibration in the gravity axis (f_z) and frequency of vibration in the perpendicular axis (f_y) have been specifically considered.

Prior to the design of the intelligent control algorithm, it is necessary to generate a look up table containing the most adequate values for the spring stiffness (K) and the damping coefficient (C) for each vibration. Considering these dependencies, an iterative process was carried out where the damping and spring values were modified for each combination of vibration in the gravity axis and in the perpendicular axis. That is, mono-frequency vibrations have been used for each axis.

With the aim of deciding the most suitable values, a criterion function has been defined in order to associate a performance index for each combination. This function

has been defined such that the displacement of the camera around the equilibrium position is decreased. In this paper, the standard deviation is used to evaluate the camera's undesired oscillations. Due to the fact that the mean is zero and since the equilibrium position of the camera is located at the origin, the standard deviation shows the camera's displacement with respect to this position. By this method, we prevent a minimum local to be chosen; it allows for a more accurate study disregarding the unwanted peaks. Equation (1) shows the standard deviation expression, x_i are the camera displacement values, N is the number of data inside each window and μ is the mean value.

$$\sigma = \frac{1}{N} \sum_{i=1}^N (x_i - \mu)^2 \quad (1)$$

Therefore, the criterion function is directly linked to the performance of the control system. Note that the values that minimize the vibration over the camera for each combination of frequencies are chosen. In this way, once the iterative process has been finished it is possible to obtain the damping and spring values which minimize the criterion function for each type of vibration. At this stage, a table with the most adequate K and C values for each vibration is generated. From now on, this table will be known as "reference table". At this point it is convenient to note that only mono-frequential vibrations signals have been considered.

In the reference table, the K value that minimizes the criterion function for the level of vibration produced by the helicopter shows very small variations, therefore it has been decided for this value to remain constant. Therefore, the damping value C will be the only parameter to be modified.

Once the reference table is obtained with the minimum values for the criterion function, it is necessary to design an intelligent system that is able to provide the most adequate values for each situation. This is, the reference table works as a data base in order to train an intelligent system. This system should be able to learn and to provide an output when confronted to an unknown input. Because of this, artificial intelligence techniques based on a training set seem to be a good choice. One suitable option could be the use of Neural Networks (Kosko, 1992), (Pajares, 2006), as their learning properties are adequate for the problem undertaken. However, determining exactly why it makes a particular decision is a daunting task because it is essentially a “black box” and it makes this approach less attractive. In this paper a Neuro-Fuzzy approach based on the scheme proposed by Jang (Jang, 1993), (Mitra, 2000), (Marichal et al. 2001) has been used. These types of methods are known as Adaptive Neuro-Fuzzy Inference Systems (ANFIS systems). In this framework, a neuro-adaptive learning method has been used. That is, a given input/output data set has been used as first step to build a Fuzzy inference system (FIS) (Zadeh, 1989), (Guijarro et al. 2009). In this paper the input set is composed of the frequencies of vibration in both axis and spring value, that

is $[f_y f_z K]$. It is a method that interprets the values in the input vector based on a set of rules and assigns values to the output vector. Specifically the output of this system provides the damping value. This involves the choice of the membership functions and fuzzy logics operators, the design of fuzzy rules, the choice of the aggregation mechanism, the involvement of the fuzzy rules (inference mechanism), and finally, the defuzzification method for obtaining a numeric output. Figure 6 shows the used ANFIS architecture.

The steps to generate the initial Fuzzy Inference system are as follows:

- The first step is to take the inputs and determine the membership degree values to each of the appropriate fuzzy sets via membership functions. The input is always a crisp numerical value and the output is a fuzzy degree of membership within the interval $[0,1]$. In this paper Gaussian membership functions have been used, determined by two parameters known as premise parameters.
- The fuzzy operator is applied and a number is obtained that represents the result of the antecedent for that rule.
- The Implication method is applied to a single number given by the antecedent, and the output is a fuzzy set represented by a membership function, which weight is a number between 0 and 1.

- The aggregation consists of the fuzzy sets that represent the outputs of each rule are combined into a single fuzzy set. The input of this process is the list of fuzzy sets that represent the outputs of each rule, and the output is a fuzzy set.
- The defuzzification process is applied, that is, the fuzzy set resulting from the process of aggregation, becomes as a number. In this paper, this process is done by weighted average as follows:

$$C = \frac{\sum_{i=1}^N \bar{w}_i z_i}{\sum_{i=1}^N \bar{w}_i} \quad (2)$$

Where C is the damping value given as system output, z_i is the output of each rule, w_i is the weight of each rule weighted and N is the total number of nodes at layer 3.

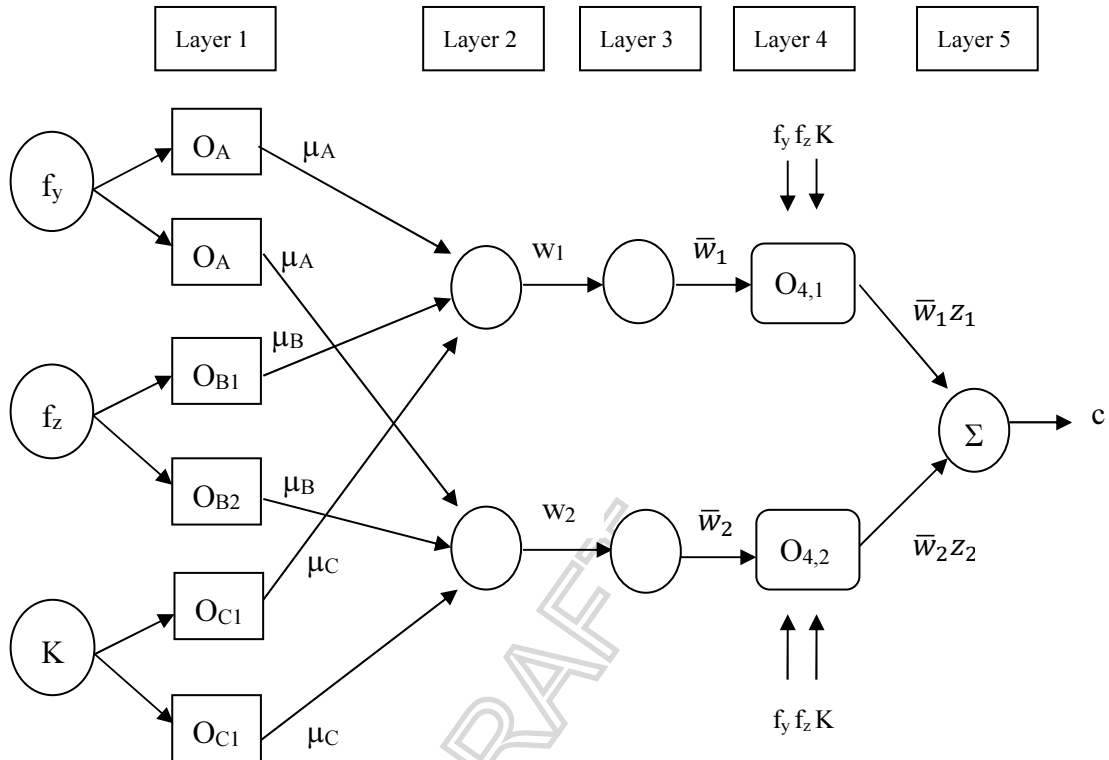


Figure 6. Architecture of the used Adaptive Neuro-Fuzzy Inference System

The ANFIS architecture (<http://www.mathworks.com/products/fuzzylogic>) has been used because it is a hybrid neural network. In our case, it has five layers, where only the layers 1 and 4 are formed by adaptive nodes. That is, they have associated parameters and they can change during the training phase. The explanation of what happens in each layer is shown below. As it was said previously the system has three inputs (f_y f_z K) each one with two membership functions, μ_{A_i} y μ_{B_j} , respectively, and an output C . Hence, this system is associated to two fuzzy if-then rules of Takagi-Sugeno type which are:

$$\text{If } f_y \text{ is } \mu_{A1} \text{ and } f_z \text{ is } \mu_{B1} \text{ and } K \text{ is } \mu_{C1} \text{ then } z_1 = p_1 f_y + q_1 f_z + r_1 K + s_1 \quad (3a)$$

$$\text{If } f_y \text{ is } \mu_{A2} \text{ and } f_z \text{ is } \mu_{B2} \text{ and } K \text{ is } \mu_{C1} \text{ then } z_2 = p_2 f_y + q_2 f_z + r_2 K + s_2 \quad (3b)$$

Where p_i, q_i, r_i, s_i are the consequent parameters.

On the first layer, each node has an output defined as:

$$O_{A,i} = \mu_{A_i}(f_y) \quad (4)$$

$$O_{B,i} = \mu_{B_i}(f_z) \quad (5)$$

$$O_{C,i} = \mu_{C_i}(K), \quad i=1, \dots, n \quad (6)$$

Where n is the number of membership functions of the inputs, two in this case and it is assumed that the three inputs have the same number of membership functions.

The second layer multiplies the input signals and each output of a node β corresponds to the consequent for each rule. Note that, it represents the weight of the conclusion of each rule.

$$w_i = \mu_{A_i}(f_y) \mu_{B_i}(f_z) \mu_{C_i}(K), \quad i=1, \dots, n; \quad (7)$$

In the third layer, the output of each node Ω corresponds to the standard weights

$$\bar{w}_i = \frac{w_i}{\sum_{i=1}^n w_i}, \quad i=1, \dots, n \quad (8)$$

The fourth layer calculates the output as a sum of the previous ones.

$$O_{4,i} = \bar{w}_i z_i = \bar{w}_i (p_i f_y + q_i f_z + r_i K + s_i), \quad i=1, \dots, n \quad (9)$$

Finally, the fifth one adds all outputs of the fourth layer and it gives as output a real number corresponding to damping value:

$$C = \sum_i \bar{w}_i z_i, i=1, \dots, n; \quad (10)$$

So far, a detailed description of the ANFIS structure has been presented. However in order to get the final ANFIS system, it is necessary to devise a selection method for parameter values.

To summarize, it can be said that the neuro-fuzzy modelling type ANFIS can be divided into three main phases: to collect input/output data in the right so it can be used by ANFIS for training, the creation of a Fuzzy System as initial structure and, the application of a learning algorithm consisting of a combination of the least-squares method and the backpropagation gradient descent method for training the ANFIS parameters. It is important to remark that these parameters are the premise and consequent parameters.

Once the method has been chosen, the ANFIS should be trained. For this purpose, the reference table obtained has been divided into two groups; the eighty percent of the data for the training phase and the rest of them to evaluate the generalization capability of the ANFIS system. The inputs training data consist of a vector containing both frequencies and the K value these minimize the movement over the camera $[f_y f_z K_{\min}]$. An additional component is necessary for the training data, and it is the desired output of the Neuro-Fuzzy. This desired output is the optimal C values for the situation

indicated by the input vector. Once the ANFIS has been trained, the rest of the data are used to validate the ANFIS system.

The trained ANFIS system is incorporated to the simulation environment in the form of a block. This block requires as input the spring value and the frequencies of the vibration signals. As the vibration signals have particular spectral characteristics, the frequencies are determined by specific blocks introduced between the fuselage vibration signal and the ANFIS block. These blocks are in charge of performing the Fast Fourier Transform (FFT) to obtain the dominant frequencies of the input signal. Figure 8 shows the FFT being calculated each 0.5 seconds and the vibrations introduced as input signals in the ANFIS controller.

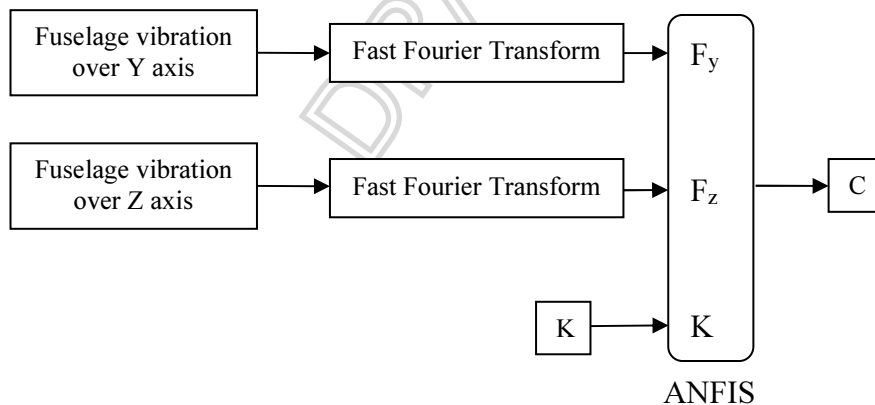


Figure 8. ANFIS controller with the adequate c value for each combination of k value and frequencies values as inputs

The next step is to introduce the semi-active control system in the simulation platform where C value is obtained by the ANFIS. The damper value changes every 0.5

seconds and as it has been explained; it depends on the type of vibration for each case. Figure 9 shows the intelligent vibration isolation system located between the point where the fuselage vibrations are received and the first body of the dynamic platform.

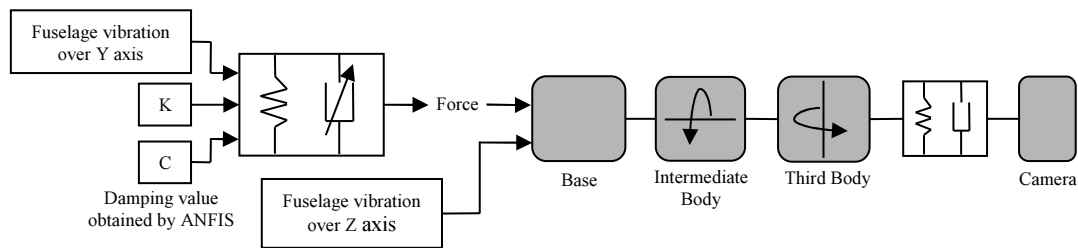


Figure 9. Intelligent vibration isolation system (grey boxes) positioned in order to reduce the vibrations.

Results

Once the semi-active isolation system and the intelligent controller have been included in the simulation platform, the vibrations from the helicopter are introduced in two blocks, one for each axis, as shown in Figure 8. Several simulations were carried out in order to study how the vibration affects the camera.

First, a vibration of 1.3 millimetres amplitude in the Y axis and in the Z axis is introduced on the vision system. It is necessary to emphasize at this point that these signals are obtained by the helicopter simulation platform presented in section 2. In order to check if the work presented in this paper improves the images captured by the camera; the camera movement is compared for each technique. In Figure 10 it can be seen appears the vibration suffered by the camera on the Y axis if the system does not have any isolation device installed. As it can be observed, at the very beginning the

signal suffers a moderated amplitude increase followed by a strong decrease, and before 0.5 seconds, its amplitude reaches values over 1.5 mm. The reason for this is the lack of an isolation system; therefore the camera will oscillate following the input vibrations generated by the helicopter model.

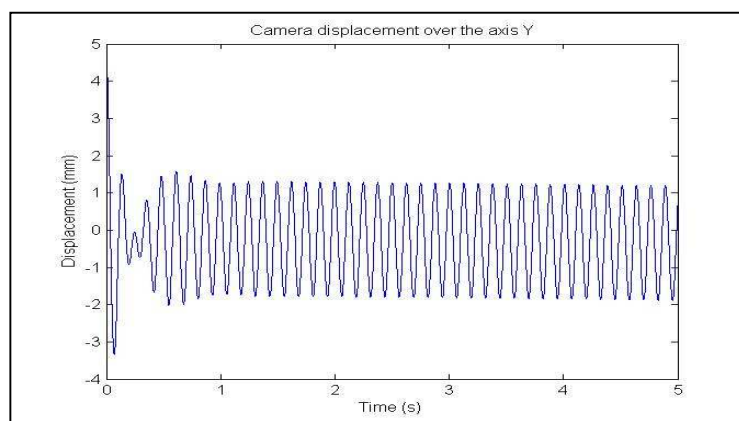


Figure 10. Vibration of the camera on the Y axis when no isolation system is implemented

Figure 11 shows a comparison of the camera behaviour if the isolation method is passive (constant spring and **damping** values); or if the proposed method with the C values chosen by ANFIS system is applied. It is important to remark that the proposed method sets new C values every 0.5 seconds and the K value is fixed to 10 N/m in both cases.

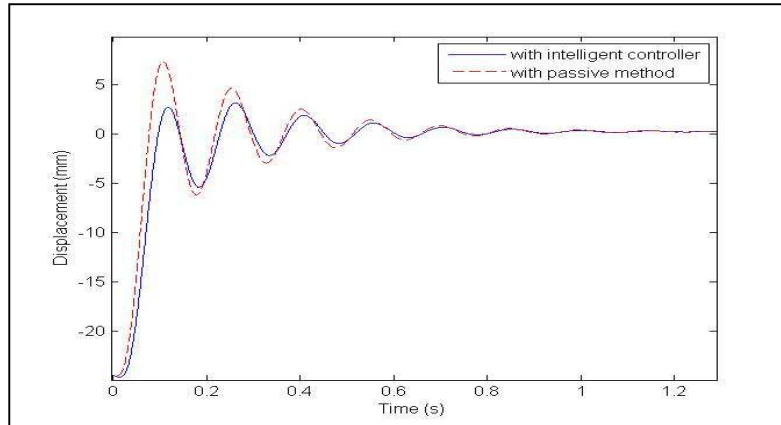


Figure 11. Comparison of vibrations in the Y axis when a passive method is used or with the proposed technique.

As it can be appreciated, after 1 second both methods perform equally, both signals converge towards the set point. Analyzing the results it is concluded that a semi-active method is better than a passive on the first 0.5 seconds. The proposed semi-active method reduces the overshoot of the vibrations suffered by the camera. This presents a substantial improvement on the vision system because the camera is kept recording continuously and in this way, more stable images can be obtained.

A second simulation with a new vibration signal from the helicopter was carried out. In this case, the introduced vibrations have lower amplitude in comparison with the previous one; however, its spectral composition of frequencies is wider. Figure 12 shows the dominant frequencies chosen by the FFT block for the case of the axis Z vibrations which are introduced in the ANFIS block shown in (Figure 8).

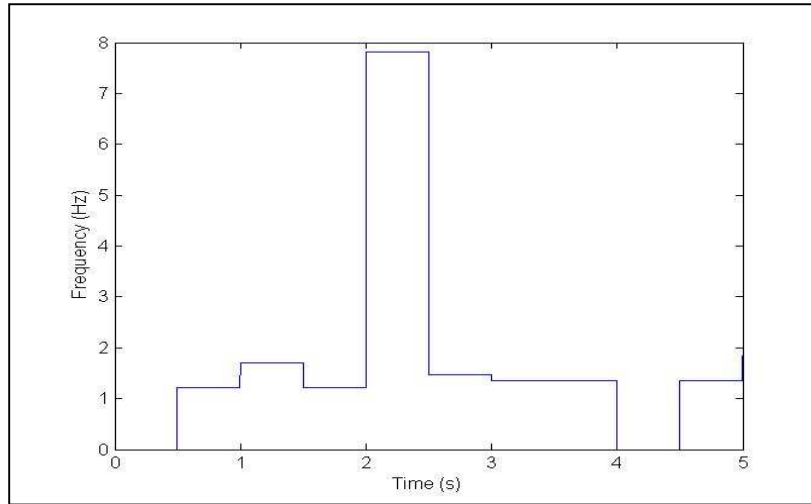


Figure 12. Dominant frequencies on the Z axis calculated each 0.5 seconds

Figure 13 shows the camera displacement in the Z axis in two cases: when a passive isolation method is used shown in (red colour) and the proposed semi-active method response, (blue colour).

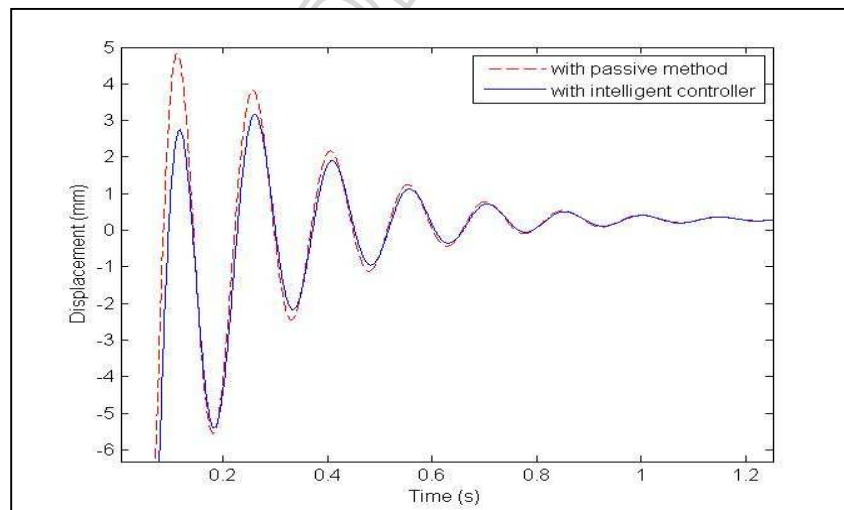


Figure 13. Comparison between camera movements on Y axis in two cases

Analyzing this result, it is seen once more that the proposed technique provides better behaviour over the first interval of time, in comparison with the traditional passive method. In this case, the vibrations cause a lower overshoot in the camera displacement in comparison to the previous results.

Conclusions

A dynamic platform with a camera and a helicopter model has been designed in Vehiclesim and Simulink/Simmechanics. This model allows studying the vibration effects produced by the helicopter over the vision system. These vibrations influence negatively on the quality of captured images because of the camera undesirable movements. This problem expresses the need for a control system that could reduce this negative influence.

In this paper an intelligent control strategy based on an ANFIS system has been proposed. Several trials have been done. The applied strategy has allowed improving the traditional passive and semi-active isolation techniques, particularly at the beginning of the vibration, during the first tenths of second. In this way a reduction in the highest peaks is achieved by low energy actions, providing a more stable vision system. The developed technique could be implemented using several semi-active actuators. In this sense, it should be pointed out that there are different current technical possibilities for semi-active device implementation such as electrorheological, magnetorheological, extension or compression principles.

The presented method provides improved images captured with a lower level of vibrations, making easier any subsequent image processing. In fact, it is important to point out that the methods used in this paper are not strongly linked to any particular platform configuration.

Acknowledgements

This work has been supported by the Spanish Government DPI2010-20751 and DPI2010-20751-C02-02 of Ministerio de Ciencia e Innovación and by the grant of the Agencia Canaria de Investigación, Innovación y Sociedad de la Información del Gobierno de Canarias, cofinanced with the European Social fund.

References

Alanoly J, Sankar S, A new concept in semi-active vibration isolation, American Society of Mechanical Engineers, Journal of Mechanisms, Transmissions, and Automation in Design 109 (1987) 242–247.

Bittanti S and Lovera M, On the zero dynamics of helicopter rotor loads, European J. Contr., 2, 1,5768, 1996.

Decker WA, Talbot PD, Tinling BE and Chen RTN. A mathematical model of a single main rotor helicopter for piloted simulation. Technical memorandum NASA 84281, NASA Ames Research Center, Moffett Field, California, September 1982

Garrad W, and Low E. Eigenspace design of helicopter flight control systems. Technical report, Dept. of Aerospace Engineering and Mechanics, Univ. of Minnesota, 1990.

Guijarro M, Pajares G. On combining classifiers through a fuzzy Multicriteria Decision Making Approach: applied to natural textured images. *Expert Syst. Appl.* 2009, 36, 7262-7269.

Heffley RK and Mních MA. Minimum complexity helicopter simulation math model. Contractor report NASA 177476. Aeroflight dynamics Directorate, U.S. Army Research and Tecnology Activity (AVSCOM), April 1988

<http://avia.russian.ee>

<http://www.carsim.com/>

Jang JR. ANFIS: Adaptive-network-based fuzzy inference system. *IEEE Trans. Syst. Man Cybern.* 1993, 23, 665-685

Jansen LM, Dyke SJ, Semi-active control strategies for MR dampers: a comparative study, American Society of Civil Engineers, *Journal of Engineering Mechanics* 126 (8) (1999) 795–803.

Johnson W, *Helicopter Theory*. Princeton, NJ: Princeton Univ. Press, 1980.

Kaloust J, Ham C and Qu Z. Nonlinear autopilot control design for a 2-DOF helicopter model, *Control Theory and Applications*, IEE Proceedings 1997, 144, 6, 612 –616.

Karnopp DC, Crosby MJ, Harwood RA, Vibration control using semi-active force generators, American Society of Mechanical Engineers, Journal of Engineering for Industry 96 (2) (1974) 619–626.

Kienitz K, Wu Q and Mansour M. Robust stabilization of a helicopter model. Proceedings of the 29th CDC, 1990, 2607 –2612.

Kosko B. Neural Networks and Fuzzy Systems: A Dynamical Systems Approach to Machine Intelligence, Prentice-Hall, Englewood Cliffs, NJ (1992).

Marichal GN, Acosta L, Moreno L, Mendez JA, Rodrigo JJ, Sigut M. Obstacle avoidance for a mobile robot: a neuro fuzzy approach. Fuzzy Sets and Systems. 2001, vol. 124, pp. 171-179

MathWorks. Matlab. Available online: <http://www.mathworks.com/products/fuzzylogic> (accessed on November 12, 2009).

Miller LR, Tuning passive, semi-active, and fully active suspension systems, in: Proceeding of the 27th Conference on Decision and Control, Austin, TX, 1988.

Mitra S, Hayashi S. Neuro-fuzzy rule generation: Survey in soft computing framework. IEEE Trans. Neural Netw. 2000, 11, 748-768

Mousseau CW, Sayers MW and Fagan D J, Symbolic quasistatic and dynamic analyses of complex automobile models, The Dynamics of Vehicles on Roads and on Railway Tracks (G. Sauvageed.), Swets and Zeitlinger, Lisse, 1992, 446-459

Narramore JC, Computational fluid dynamics development and validation at Bell Helicopter. Textron Bell Helicopter, Fort Worth, TX. In AGARD, Aerodynamics and Aeroacoustics of Rotorcraft 13, (SEE N96-13582 02-01), 1995.

Padfield GD. Helicopter flight dynamics: the theory and application of flying qualities and simulation modelling. Oxford: Blackwell, 1996

Pajares G. A Hopfield Neural Network for Image Change Detection. IEEE Trans. Neural Netw. 2006, 17, 1250-1264

Rakheja S, Sankar S, Effectiveness of “on-off” damper in isolation dynamical systems. Shock and Vibration Bulletin 57 (1986) 147–156.

Rakheja S, Sankar S, Vibration and shock isolation performance of a semi-active “on-off” damper, American Society of Mechanical Engineers, Journal of Vibration, Acoustics, Stress, and Reliability in Design 107 (1985) 398–403.

Sayers MW (1999) Vehicle models for RTS applications. Vehicle System Dynamics 32(4-5): 421-438

Sharp RS, Evangelou S and Limebeer DJN, Advances in the modeling of motorcycle dynamics, Multibody System Dynamics 12(3), 2004, 251-283

Sharp RS, Evangelou S and Limebeer DJN, Multibody aspects of motorcycle modelling with special reference to Autosim, Advances in Computational Multibody Systems, J. G. Ambrósio (Ed.), Springer- Verlag, Dordrecht, The Netherlands, 2005, 45-68

Simulink ® Available online <http://www.mathworks.com/products/simulink/>

Steele Jr. and Guy L. COMMON LISP: The language. Digital Press. Burlington, Mass, 1984

Tomás-Rodríguez M, Sharp R, Automated Modeling of Rotorcraft Dynamics with Special Reference to Autosim, Automation Science and Engineering, 2007. CASE 2007. IEEE International Conference, 2007, Pages: 974-979

Tomás-Rodríguez M. “Helicopter rotor dynamics modelling”, MPhil Thesis, Imperial College, 2008.

Verdult V, Lovera M and Verhaegen M. Identification of linear parameter-varying state-space models with application to helicopter rotor dynamics, International Journal of Control, 77, 13, Sep 2004, 1149 - 1159.

Wu X, Griffin MJ, A semi-active control policy to reduce the occurrence and severity of end-stop impacts in a suspension seat with an electrorheological fluid damper, Journal of Sound and Vibration 203 (5) (1997) 781–793.

Zadeh LA. Knowledge representation in fuzzy logic. IEEE Trans. Knowl. Data Engin. 1989, 1, 89-100.